Stability of Thiol-Passivated Gold Particles at Elevated Temperatures Studied by X-ray Photoelectron Spectroscopy

Michael Büttner,*,† Thomas Belser,‡ and Peter Oelhafen†

Institute of Physics, Klingelbergstr. 82, 4056 Basel, Switzerland, and Department of Chemistry, St. Johanns-Ring 19, 4056 Basel, Switzerland

Received: August 20, 2004; In Final Form: November 26, 2004

The thermal stability of thiol-passivated gold colloids has been studied by means of X-ray photoelectron spectroscopy. Different colloids were chemically synthesized with thiol lengths from 3 to 8, and 16 carbon atoms. Depending on the synthesis parameters, the mean gold particle size varied from 1.6 to 4.9 nm for the particular colloid. Temperature-dependent measurements revealed a general tendency of shells with longer thiol chains (>5 carbon atoms) to be more stable in terms of desorption but to show a X-ray radiation-induced damage, which was absent with shorter thiols. Additionally, the self-assembling properties of the colloids were characterized by TEM, showing differences as a function of the chain lengths.

1. Introduction

There is an increasing interest in nanoparticles and their application in physics, chemistry, and biology. Nanometer-sized particles can show different or even new features in their electronic properties compared to the bulk material, mainly due to two factors. First, by reducing the cluster size, electron quantum confinement effects play an increasingly important role. Second, the contribution of surface atoms to the electronic properties increases with decreasing cluster diameter. This makes nanoparticles interesting for a variety of electronic applications, such as single-electron transistors (SET),[1,2] diodes,[3]and quantum dots.[4,5] Ordered arrays of metal nanoparticles exhibit optical properties that can be controlled via particle size and interparticle distance.[6−8] To achieve this, the use of organic-shell passivated metal clusters is of great benefit. Organic shells around the particles play a crucial role in the self-assembly, because such a mechanism is mainly driven by the interacting forces of the shell molecules.[9] The large range of chemical synthesis methods available enables choice of the passivating shell from a variety of molecules with different lengths and functional groups. For example, this enables to control the interparticle distance. However, restrictions in the choice of the chain lengths apply in the case of thiol molecules.[10] The particle size (another important parameter) can also be controlled during synthesis within certain limits imposed by the applied method.[11] Recent reports have shown the feasibility of removing the organic shell by means of oxygen and hydrogen radio frequency (RF) plasmas. This procedure does not alter the geometric arrangement of the particles and results in an array of naked metal particles.[12] In summary, as nanoparticle research is a very active field, better knowledge is necessary to be able to tailor nanoparticle systems with particular desired properties.

The aim of this work was to investigate the influence of temperature on the stability of thiol-passivated gold nanoparticles with different thiol chain lengths. For the first time, a complete range of thiol lengths starting from 3 (C3) up to 8 (C8), and 16 (C16) carbon atoms has been investigated. Theoretical works based on computer calculations using density functional theory (DFT) mainly focus on short-chain thiols (typically 3−4 carbon atoms) due to the large amount of calculation time necessary when treating longer chains. On the contrary, experimental results are obtained mostly from thiol chain lengths of 8 and more carbon atoms. Colloids with mean particle diameters ranging from 1.6 to 4.9 nm have been synthesized and thiol-passivated by a well-established two-phase method. X-ray photoelectron spectroscopy (XPS) has been used to monitor the changes in the sulfur-to-gold ratio with increasing temperature.

2. Experimental Section

The gold cluster compounds were synthesized using a modified literature procedure from Murray et al.[13] All glassware used for the preparation and storage of colloidal gold was treated with aqua regia, rinsed with deionized water, cleaned in a bath consisting of seven parts concentrated sulfuric acid and three parts 30% hydrogen peroxide (piranha solution), rinsed again with deionized water, and dried for 12h at 120 °C. All reactions were carried out under inert atmosphere and in darkness. To a vigorously stirred solution (1200 rpm) of $HAuCl_4 \cdot xH_2O$ (containing 49% Au; 3.00 g, 7.41 mmol) in deionized H_2O (240 mL) was added a solution of tetraoctylammoniumbromide (4.50 g, 8.23 mmol) in freshly distilled toluene (165 mL). The yellow $HAuCl_4 \cdot xH_2O$ aqueous solution quickly cleared and the toluene phase became orange/red as the $AuCl_4^-$ was transferred into it. This mixture was shaken several times in order to obtain complete removal of color from the aqueous phase. The organic phase was isolated and the corresponding thiol (1.48 mmol) was added to the solution. The resulting solution was cooled to 0 °C. The solution was vigorously stirred (1200 rpm), and $NaBH_4$ (3.10 g, 82.0 mmol) in deionized water (200 mL) was added over 15 s. The colloids were transformed instantaneously as witnessed by the color change of the solution from red to black. The organic phase was collected and the solvent was removed to 20 mL on a rotary evaporator (the water bath should not exceed 30 °C to prevent partial product decomposition). The black product was suspended in ethanol (300 mL) and briefly sonicated to ensure complete dissolution of byproducts. The

* Corresponding author. E-mail: Michael.Buettner@unibas.ch.
† Institute of Physics.
‡ Department of Chemistry.

10.1021/jp0462355 CCC: $30.25
Published on Web 03/04/2005

mixture was kept at −60 °C for 48 h to effect precipitation. The precipitated colloids were collected on a glass filtration frit and washed twice with ethanol (150 mL) and twice with acetone (100 mL). The black material was dried in vacuo for 1 h to give 1.8 g thiol-passivated gold nanoparticles, free of significant residual thiol. The purity of the sample was determined by the absence of resonance due to free alkanethiol in the ^{1}H NMR spectrum ($CDCl_3$), in particular the α-CH_2 resonance at 2.5 ppm. The IR spectra no longer exhibited the characteristic ν_{asym}(SH) band in the region of 2563 cm^{-1}. The powder consisting of thiol-passivated gold clusters was dissolved in toluene with a concentration of less than 0.5 mg/mL. For each synthesized colloid, TEM imaging was carried out in order to measure the particle size. For the TEM sample preparation, the gold colloid solution was drop-deposited onto a carbon-coated copper grid and then transferred into the TEM after the solvent was completely evaporated. A FEI/Philips Morgagni 268D TEM was used with a Digicam Megaview II camera for imaging. As the particles were not size-selected, a size dispersion of about ± 20% was unavoidable in each sample due to the synthesis method. Particles of different mean diameters with thiol chain lengths from 3 to 8, and 16 carbon atoms, respectively, were used for the experiments. We included two samples with the same thiol (C8) shell, but different mean diameter (1.6 nm and 3.1 nm), in order to study the influence of particle size on the experimental results.

XPS core level measurements took place in UHV conditions, with a base pressure of about 1×10^{-9} mbar. Mg K_α nonmonochromatized X-rays with a main photon energy of 1253.6 eV were used as the excitation source throughout the whole series of measurements, and the expelled photoelectrons were analyzed with a Leybold EA11 hemispherical mirror energy analyzer with a pass energy of 30 eV. The typical energy resolution (fwhm) of this setup was about 0.9 eV. A freshly leaved HOPG substrate with drop-deposited colloid solution (typically 5−10 μL) was transferred into the measurement chamber, after the solvent evaporated completely. The sample was mounted on a sample holder with a small resistive button heater to allow heating in vacuo between measurements. The heater was equipped with a thermocouple for temperature control. For the heating step, the sample was brought to the desired temperature, which was maintained for 5 min. After cooling, the sample was measured at room temperature. Such XPS measurements take about 3 h each. The Au4f and S2p core level lines were decomposed with a Doniach-Sunjic line shape using the Levenberg−Marquardt fitting algorithm. From these decompositions the sulfur-to-gold ratio was calculated.

3. Results and Discussion

Figure 1 shows two typical examples of S2p spectra, which are representative for the whole ensemble of samples. While in the case of C3 the spectrum consists of a single spin doublet (doublet A) with a $S2p_{3/2}$ binding energy of 162.4 eV (associated to sulfur−gold bonding[14]), in the case of C16 the spectrum is composed of two doublets (A and B), with a $S2p_{3/2}$ binding energy of 163.5 eV for doublet B. The relative intensities between doublet A and doublet B were not fixed, but evolved during the experiments in favor of doublet B. Based on the existence or nonexistence of doublet B in the corresponding decomposed S2p spectrum, we divided our samples into two groups: short thiols with no doublet B (C3, C4, and C5) and long thiols with doublet B (C6−C8, and C16). According to the literature, doublet B can be attributed to a sulfur species that appears with increasing X-ray radiation time, indicative of

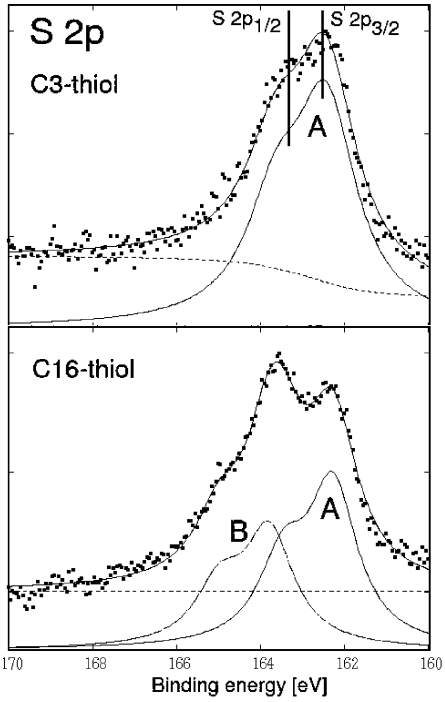

Figure 1. Typical decompositions of the S2p core-level spectrum for short thiols (represented by C3) and long thiol (C16). Doublet A is asocciated with a S−Au bond, while doublet B indicates a X-ray radiation-induced sulfur species, i.e., progressive thiol shell damage. In contrast to long thiols (C6−C8, and C16), short thiols (C3, C4, and C5) showed no radiation-induced doublet B.

damage to the thiol shell,[15,16] although there is still discussion about the nature of this species, e.g., disulfide or dialkyl sulfide. To verify this, we irradiated selected samples (C3, C4, C8, C16) at room temperature with X-ray radiation for 17 h, and XPS measurements were taken every 4 h to monitor changes in the S2p spectra. To summarize the results of this investigation, the relative intensity of doublet B to doublet A increased gradually as a function of radiation time: From 0.1 to 0.8 for C8, and from 0.2 to 1.2 for C16. Samples C3 and C4 did not evolve a doublet B. It can be concluded that the X-ray radiation leads to progressive S−Au bond breaking and the creation of the new sulfur species. This will be accounted for in our interpretation of the experimental results. As S−C bond scission is unlikely to occur due to its high binding energy, it is reasonable to use sulfur as a monitor for the degradation of the thiol shell.

Figure 2 shows the sulfur-to-gold (S/Au) ratio as a function of the annealing temperature. As previously mentioned, the curves are displayed in separate graphs, based on the existence of doublet B. The upper part (a) consists of samples with short thiols of five or fewer carbon atoms. The prominent feature is a strong decrease of the S/Au ratio in a region between 90 °C and 140 °C. This behavior marks the beginning of a temperature-induced desorption of sulfur. The lower part (b) shows samples with long thiols of six or more carbon atoms. Unlike the case of shorter thiol chains, the samples show much smaller variations in the S/Au ratio up to 160 °C, except for sample C7. Going to higher temperatures, a strong decrease can be observed, which is associated with sulfur desorption. This was also confirmed by additional thermogravimetric and differential calorimetry measurements performed on a octanethiol (C8) sample (not shown).

In Figure 3 we see the development of the S/Au ratio for doublet A, which shows the fraction of thiol still attached to the gold particle. Data points for C3, C4, and C5 are omitted,

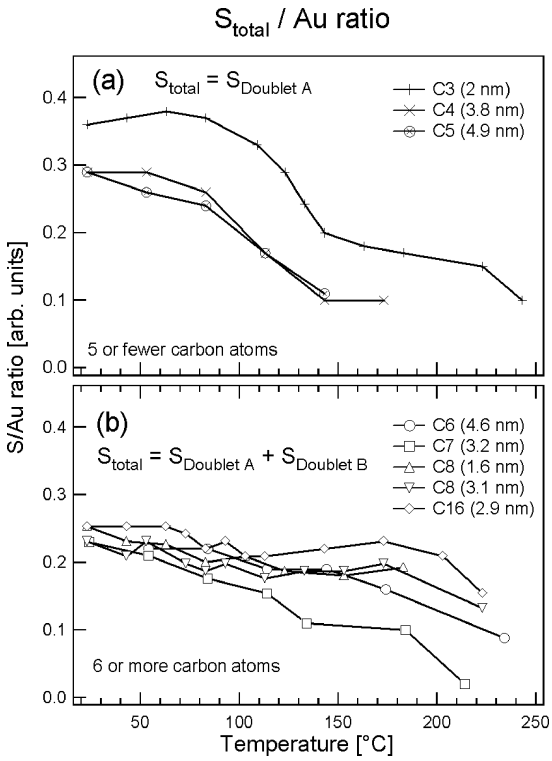

Figure 2. The S/Au ratio as determined by XPS as a function of the temperature. Passivating shells with short thiols (a) show desorption between 90 and 140 °C; shells with longer thiols (b) desorb above 160 °C.

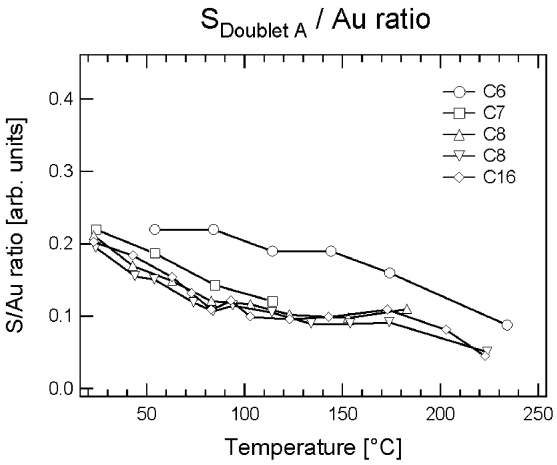

Figure 3. The S/Au ratio for doublet A (S−Au bond) indicates progressive thiol shell damage between room temperature and 160 °C. It is caused by continuous X-ray radiation and is not temperature-related. Short thiols are omitted, as they did not exhibit radiation-induced doublet B.

as they are identical to Figure 2a. Due to low signal-to-noise ratio of the S2p spectrum, a decomposition of the two doublets cannot be given above 120 °C. A progressive immediate decrease of the S/Au ratio with increasing temperature can be observed. Taking into account the previously addressed effect of X-ray radiation upon the S2p spectra, this decrease can be interpreted as S−Au bond breaking induced by X-ray radiation and not as thiol desorption induced by the elevated temperature. As was shown in Figure 2b, for most samples, the S/Au ratio for the total amount of sulfur varied little over the temperature range, where the damage took place. In conclusion, this means that short thiol shells show no degradation with X-ray radiation but desorb between 90 °C and 140 °C. On the other hand, long

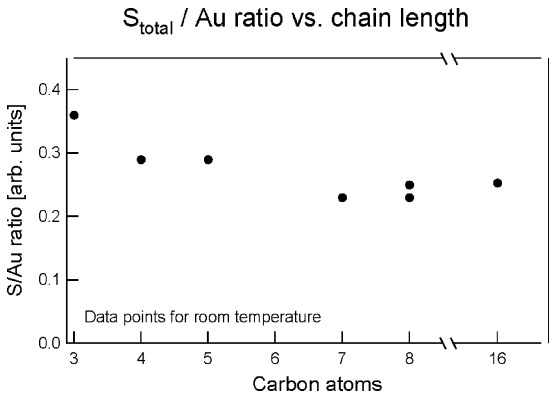

Figure 4. The S/Au ratio as a function of the thiol length. The increase for short chains may indicate a higher thiol density on the gold surface.

thiol shells are stable up to temperatures of 160 °C but show S−Au bond breaking due to X-ray radiation damage. The mean particle diameter of the examined samples did not significantly affect the results, as was confirmed by the two C8 samples. According to theoretical calculations, the S−Au binding energy should not be affected by variation of the thiol chain length (for C>2).[17] However, our results show different reaction (in terms of radiation-induced damage) to X-ray radiation for short and long thiol chains. The changes in desorption temperature reflect the stabilizing forces between the thiol molecules, which increase with longer chain lengths.[18,19] Additionally, it has been reported that thiols of less than five carbon atoms produce colloids that tend to degrade over several weeks, whereas colloids with longer chains can be kept under ambient conditions for months without showing any sign of degradation.[20]

The possibility of thiol adsorption on the HOPG substrate was checked experimentally with a pristine HOPG sample in a vacuum chamber exposed to thiol vapor. For this experiment an air-cleaved HOPG substrate was exposed to a hexadecanethiol (C16) atmosphere of 1×10^{-6}mbar for 1 h. The thiol was introduced in the chamber through a leak valve. Afterward, the substrate was checked with XPS, and no traces of sulfur could be detected, which eliminated the possibility that the thiol chains may have attached to the HOPG surface after S−Au bond breaking. Therefore, we propose that the thiol shell is still located around the gold core even under increasing X-ray radiation damage.

Nothing has been said yet about the Au4f binding energies, which have also been evaluated. We cannot give a satisfactory interpretation of these results yet. The Au4f binding energy of the freshly prepared gold particles was shifted to higher binding energies with decreasing particle diameter, about 0.2 eV for C8 (1.6 nm). At a first approximation, this can be regarded as final-state effects caused by the photoemisson process.[21] However, during the heating experiments, the binding energy shifted back toward the bulk gold value. Following our conclusions about the stability of the passivating shell, particle coalescence is unlikely to occur. Furthermore, thiol adsorption experiments on small gold particles (a few hundred atoms, estimated from Au5d splitting) performed in our vaccum chamber showed a shift of the Au4f doublet to higher binding energies of ≈0.4 eV upon adsorption of hexadecanethiol (C16). It is questionable whether the shift observed with the gold colloids is induced by the mentioned final-state effect alone. A detailed examination therefore must be postponed to a later publication.

The S/Au ratio (S_{total}) as a function of the thiol length is shown in Figure 4. The data points were taken from Figure 2 at room temperature. An increased S/Au ratio can be observed for the

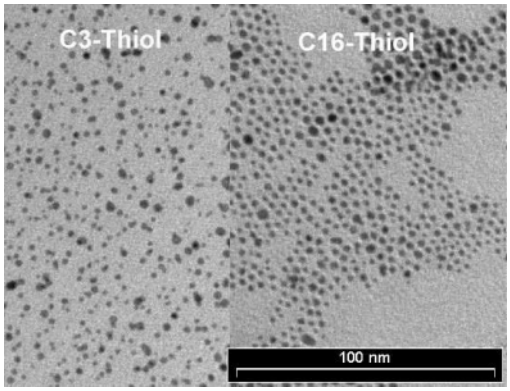

Figure 5. The two TEM images show the influence of the thiol shell upon the self-assembling properties. Left: propanethiol (C3), right: hexadecanethiol (C16).

shortest thiol chains. A possible explanation for this would be that the thiol chain density on the gold cluster surface is dependent on the chain length, e.g., through different spacial orientation. This means a higher thiol density with shorter thiol length. An effect of the particle size can be neglected, as the data for the two C8 samples match well. This result stands in contrast to earlier studies of thiol monolayers on flat gold substrates, where an increase of thiol packing density with increasing chain length was observed.[22] Influence of the different thiol chain lengths (namely variation of the S/Au ratio because of different sampling depths for the photoelectrons) can be ruled out as this would lead to an increased S/Au ratio with longer thiols. This discrepancy cannot be cleared within the scope of this work and needs more investigation.

Figure 5 shows the TEM images for samples with the shortest (C3) and longest (C16) thiol chain. While the C3-thiol-passivated particles are randomly scattered, the C16-thiol-passivated particles form dense two-dimensional islands. The main driving factor for the self-assembling mechanism has its origin in the interaction force between the hydrocarbon chains.[23] They play a prominent role in the crystallization process and can outweigh the van der Waals forces between the metal nanocores by 2 orders of magnitude.[9] We could speculate as follows: the propanethiol molecule shell only interacts weakly with the shells of other nanoparticles, thus exhibiting only small tendency to crystallize into denser islands. The hexadecanethiol shells on the other hand give rise to a much stronger interaction force between the passivating shells, which leads to a strong crystallization force. As the colloids had to be drop-cast on a carbon-coated grid for TEM imaging and not on an HOPG substrate as before, further examination will be necessary to study the particle organization on HOPG.

4. Conclusion

We have studied the influence of the chain length upon the thermal stability of the passivating thiol shell of gold nanoparticles deposited on HOPG. The ratio of sulfur to gold obtained by XPS measurements was used to monitor the degradation of the thiol shell as a function of temperature. Our results showed that short thiols (C3, C4, and C5) begin to desorb from the sample between 90 and 140 °C, whereas for long thiols (C6−C8, and C16) this threshold is around 160 °C. The effect of progressive thiol shell damage (S−Au bond breaking) through continuous X-ray radiation was observed with long thiol molecules but was absent with short thiols. Examination of the decomposed S2p spectra led to the conclusion that the thiol molecules stay located around the gold core, even under X-ray radiation damage. Comparing the S/Au ratio in terms of thiol chain length, an increased value for short thiols may indicate an higher thiol density on the gold core. The comparison of two C8 samples with different particle sizes indicated no influence of the diameter upon the experimental results. According to preliminary investigations, the self-assembling properties of the colloids are highly affected by the thiol length, as shown with TEM images of C3 and C16 colloids. The particles are randomly scattered with a high interparticle distance for C3. In contrast to this, the C16 colloid arranges in two-dimensional islands.

Acknowledgment. Financial support was granted by the Swiss National Fund (SNF) and the National Center of Competence in Research (NCCR) "Nanoscale Science". We also thank Teresa de los Arcos, Cara Humphrey, and Jonathan Medlock for reviewing the manuscript and Tamara Fretz (ZMB, University Basel) for providing the TEM images and doing the particle size analysis.

References and Notes

(1) Wang, B.; Wang, H.; Li, H.; Zeng, C.; Hou, J. G. *Phys. Rev. B* **2000**, *63*, 35403.
(2) Sato, T.; Ahmed, H.; Brown, D.; Johnson, B. *J. Appl. Phys.* **1997**, *82*, 696.
(3) Torma, V.; Reuter, T.; Schumann, M.; Schmid, G. *Chem. Phys. Chem.* **2001**, *8/9*, 546.
(4) Barnett, R.; Cleveland, C.; Häkkinen, H.; Landman, U. *Eur. Phys. J. D* **1999**, *9*, 95.
(5) Park, K.-H.; Shin, M.; Ha, J. S.; Soo Yun, W.; Ko, Y.-J. *Appl. Phys. Lett.* **1999**, *75*, 139.
(6) Linden, S.; Kuhl, J.; Giessen, H. *Phys. Rev. Lett.* **2001**, *86*, 4688.
(7) Lamprecht, G.; Schider, G.; Lechner, R.; Ditlbacher, H.; Aussenegg, F. *Phys. Rev. Lett.* **2000**, *84*, 4721.
(8) Felidj, N.; Aubard, J.; Levi, G. *Phys. Rev. B* **2002**, *65*, 75419.
(9) Gutierrez-Wing, C.; Santiago, P.; Ascencio, J.; Camacho, A.; Jose-Yamacan, M. *Appl. Phys. A* **2000**, *71*, 237.
(10) Martin, J.; Wilcoxon, J.; Odinek, J.; Provencio, P. *J. Phys. Chem. B* **2000**, *104*, 9475.
(11) Leff, D.; Ohara, P.; Heath, J.; Gelbart, W. *J. Phys. Chem.* **1995**, *99*, 7036.
(12) Boyen, H.-G.; Herzog, Th.; Kästle, G. *Phys. Rev. B* **2002**, *65*.
(13) Hostetler, M.; Wingate, J.; Zhong, C.-J.; Murray, R. *Langmuir* **1998**, *14*, 17.
(14) Ishida, T.; Choi, N.; Mizutani, W. *Langmuir* **1999**, *15*, 6799.
(15) Zerulla, D.; Chasse, T. *Langmuir* **1999**, *15*, 5285.
(16) Heister, K.; Zharnikov, M.; Grunze, M. *Langmuir* **2001**, *17*, 8.
(17) Krüger, D.; Fuchs, H.; Rousseau, R.; Marx, D.; Parrinello, M. *J. Chem. Phys.* **2001**, *115*, 4776.
(18) Terrill, R.; Postlethwaite, T.; Chen, C.; Murray, R. *J. Am. Chem. Soc.* **1995**, *117*, 12537.
(19) Badia, A.; Singh, S.; Lennox, R. B. *Chem. Eur. J.* **1996**, *2*, 359.
(20) Brust, M.; Kiely, C. *Colloids Surf. A* **2002**, *202*, 175.
(21) DiCenzo, S. B.; Berry, S. D.; Hartford, E. H. *Phys. Rev. B* **1988**, *38*, 8465.
(22) Porter, M.; Bright, T.; Allara, D.; Chidsey, C. *J. Am. Chem. Soc.* **1987**, *109*, 3559.
(23) Luedtke, W. D.; Landman, U. *J. Phys. Chem.* **1996**, *100*, 13323.